Site percolation on square and simple cubic lattices with extended neighborhoods and their continuum limit

Zhipeng Xun [1,*] Dapeng Hao [1,†] and Robert M. Ziff [2,‡]

[1] *School of Material Sciences and Physics, China University of Mining and Technology, Xuzhou 221116, China*

[2] *Center for the Study of Complex Systems and Department of Chemical Engineering, University of Michigan, Ann Arbor, Michigan 48109-2800, USA*

(Received 20 October 2020; accepted 22 January 2021; published 12 February 2021)

By means of extensive Monte Carlo simulation, we study extended-range site percolation on square and simple cubic lattices with various combinations of nearest neighbors up to the eighth nearest neighbors for the square lattice and the ninth nearest neighbors for the simple cubic lattice. We find precise thresholds for 23 systems using a single-cluster growth algorithm. Site percolation on lattices with compact neighborhoods of connected sites can be mapped to problems of lattice percolation of extended objects of a given shape, such as disks and spheres, and the thresholds can be related to the continuum thresholds η_c for objects of those shapes. This mapping implies $zp_c \sim 4\eta_c = 4.51235$ in two dimensions and $zp_c \sim 8\eta_c = 2.7351$ in three dimensions for large z for circular and spherical neighborhoods, respectively, where z is the coordination number. Fitting our data for compact neighborhoods to the form $p_c = c/(z+b)$ we find good agreement with this prediction, $c = 2^d\eta_c$, with the constant b representing a finite-z correction term. We also examined results from other studies using this fitting formula. A good fit of the large but finite-z behavior can also be made using the formula $p_c = 1 - \exp(-2^d\eta_c/z)$, a generalization of a formula of Koza, Kondrat, and Suszcayński [J. Stat. Mech.: Theor. Exp. (2014) P11005]. We also study power-law fits which are applicable for the range of values of z considered here.

DOI: 10.1103/PhysRevE.103.022126

I. INTRODUCTION

Percolation is an important model in statistical physics [1,2] because of its fundamental nature and its many practical applications, like liquids moving in porous media [3,4], forest fires problems [5,6], and epidemics [7,8]. Consequently, researchers have devoted considerable effort to study it and many valuable advances have been made.

Numerous lattice models have been widely investigated to find the percolation threshold p_c, which is a central quantity of interest in this field, along with the critical exponents and other related quantities. Among these lattice models, percolation on lattices with extended neighborhoods is of interest due to many reasons. (Here we define "neighborhoods" as the region of sites that connect to a given site by the extended-range bonds.) For example, some problems related to 2D (two-dimensional) bond percolation with extended neighborhoods may provide a way to understand the spread of coronavirus from a percolation point of view. In fact, many types of systems can be studied with extended neighbors, because the coordination number z can be varied over a wide range. Bond percolation with extended neighbors has long-range links similar to small-world networks [9] and is similar to spatial models of the spread of epidemics via long-range links [10]. Site percolation on lattices with extended neighborhoods is related to problems of adsorption of extended objects on a lattice, such as disks and squares [11,12]. In addition, this kind of lattice structure lies between discrete percolation and continuum percolation, so further study will be helpful to establish the relationship between these two problems [11–13].

The study of percolation on lattices with extended ranges of the bonds goes back to the "equivalent neighbor model" of Dalton, Domb, and Sykes in 1964 [13–15], and many papers have followed since. Gouker and Family [16] studied extended-range site percolation on compact regions in a diamond shape on a square lattice, up to a lattice distance of 10. Jerauld, Scriven, and Davis [17] studied both site and bond percolation on body-centered cubic lattices with nearest and next-nearest-neighbor bonds. Gawron and Cieplak [18] studied site percolation on face-centered cubic lattices up to fourth nearest neighbors. In a comprehensive work, d'Iribarne, Rasigni, and Rasigni [19–21] studied site percolation on all 11 of the Archimedian lattices ("mosaics") with extended-range connections up to the 10th nearest neighbors. Malarz and Galam [22,23] introduced the idea of "complex neighborhoods" where various combinations of neighbors, not necessarily compact, are studied, and this has been followed up by many subsequent works in two, three, and four dimensions [24–28]. Koza and collaborators [11,12] studied percolation of overlapping objects on a lattice, and this problem can be mapped to extended-range site percolation as discussed below. Most of the earlier work involved site percolation, but bond percolation has also been studied to high precision in several recent works [29–33]. A theoretical analysis of finite-z corrections for the bond thresholds has recently been given by Frei and Perkins [34]. Some related work on polymer systems has also appeared recently [35].

*zpxun@cumt.edu.cn
†dphao@cumt.edu.cn
‡rziff@umich.edu

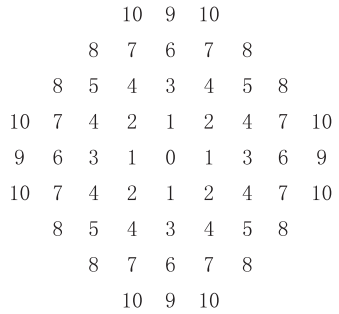

FIG. 1. Neighbors of a central site ("0") on a square lattice, up to 10th nearest neighbors.

Note that here we call this problem "extended-range percolation" rather than "long-range percolation" because the latter term has frequently been used to indicate infinte-range links, with a decreasing size distribution such as by a power law (although several of the extended-range papers referenced here [16,21] use the "long-range" name). As mentioned above, other names in the literature include "equivalent neighbors," [15], "medium-range percolation [36], and "complex neighborhoods" [22].

Correlations between percolation thresholds p_c and coordination number z and other properties of lattices have long been discussed in the percolation field. Domb [13] argued that for extended-range site percolation, the asymptotic behavior for large z could be related to the continuum percolation threshold η_c for objects of the same shape as the neighborhood of the extended-range connections, and this argument has also been advanced by others [11,12,21]. As discussed below, for large z this implies that

$$p_c \sim \frac{2^d \eta_c}{z}, \tag{1}$$

where d is the number of dimensions. Here η_c is the total volume of adsorbed objects of the shape of neighborhood, including overlapping volumes, per unit volume of the system, at criticality in continuum percolation. In contrast, for bond percolation, one expects that Bethe-lattice behavior to hold for large z,

$$p_c \sim \frac{1}{z-1}, \tag{2}$$

because for large z and low p, the chance of hitting the same site twice is vanishingly small and the system behaves basically like a tree. Thus, in both cases, one expects $p_c \sim z^{-1}$ as $z \to \infty$, but with different coefficients.

In this paper, we focus on site percolation on the square (SQ) and the simple cubic (SC) lattices, with various extended neighborhoods, based on Monte Carlo simulation, using a single-cluster growth algorithm. Diagrams of the SQ and SC lattices showing neighbors up to the 10th and ninth nearest neighbors, respectively, are shown in Figs. 1 and 2, and the distances and multiplicities are shown in Tables I and II. Precise site percolation thresholds are obtained, and fits related to the asymptotic behavior in Eq. (1) as well as power-law fits are discussed.

Here we use the notation SC-$a, b, \ldots$ to indicate a simple cubic lattice with bonds to the ath nearest neighbor, the

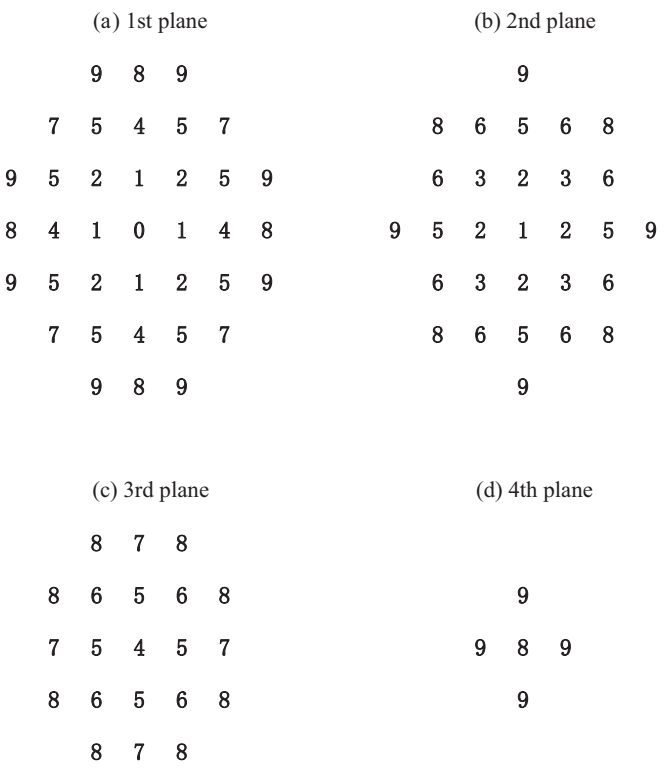

FIG. 2. Four planes of the simple cubic lattice showing neighbors up to the ninth nearest neighbors surrounding the site marked ("0") on the first plane.

bth nearest neighbor, etc., and likewise for the square lattice (SQ). Other notations that have been used include $(a, b, \ldots)$ [14], $(a\text{NN} + b\text{NN} + \cdots)$ [22,26], $[(a+1)\text{N} + (b+1)\text{N} + \cdots]$ [24]. That is, in Ref. [24], "3N" signifies the next-nearest neighbor (NNN), a distance $\sqrt{2}$ from the origin, while in Ref. [22] that neighbor is called "2NN" indicating the second nearest neighbor. We also call the second nearest neighbor "2" as shown in Figs. 1 and 2.

The remainder of the paper is organized as follows. Section II describes the numerical method and the underlying

TABLE I. Nearest-neighbor distances r and multiplicities on the square lattice.

Neighbor	r^2	Number	Total z
1	1	4	4
2	2	4	8
3	4	4	12
4	5	8	20
5	8	4	24
6	9	4	28
7	10	8	36
8	13	8	44
9	16	4	48
10	17	8	56
11	18	4	60
12	20	8	68
13	25	12	80

TABLE II. Nearest-neighbor distances r and multiplicities on the cubic lattice.

Neighbor	r^2	Number	Total z
1	1	6	6
2	2	12	18
3	3	8	26
4	4	6	32
5	5	24	56
6	6	24	80
7	8	12	92
8	9	30	122
9	10	24	146
10	11	24	170
11	12	8	178
12	13	24	202
13	14	48	250

theory. Section III gives the threshold results. A detailed discussion of the results and a discussion of other works is given in Sec. IV, and in Sec. V we present our conclusions.

II. METHOD AND THEORY

A. Simulation method

We use a single-cluster growth algorithm described in previous papers [31,32,37]. We generate many samples of individual clusters and put the results in bins in ranges of $(2^n, 2^{n+1} - 1)$ for $n = 0, 1, 2, \ldots$. Clusters still growing when they reach an upper size cutoff are counted in the last bin. From the values in the bins, we are able to find the quantity $P_{\geqslant s}$, the probability that a cluster grows greater than or equal to size s, for $s = 2^n$. From the behavior of this function, we can determine if we are above, near, or below the percolation threshold, as discussed below.

B. Basic theory

The method mentioned above depends on knowing the behavior of the size distribution (number of clusters of size s) $n_s(p)$. In the scaling limit, in which s is large and $(p - p_c)$ is small such that $(p - p_c)s^\sigma$ is constant, $n_s(p)$ behaves as

$$n_s(p) \sim A_0 s^{-\tau} f[B_0(p - p_c)s^\sigma], \tag{3}$$

where τ, σ, and $f(x)$ are universal, while A_0 and B_0 are lattice-dependent "metric factors." At the critical point, Eq. (3) implies $n_s(p_c) \sim A_0 s^{-\tau}$ assuming $f(0) = 1$. For finite s at p_c, there are corrections to this of the form

$$n_s(p_c) \sim A_0 s^{-\tau}(1 + C_0 s^{-\Omega} + \cdots). \tag{4}$$

The probability that a point belongs to a cluster of size greater than or equal to s is given by $P_{\geqslant s} = \sum_{s'=s}^{\infty} s' n_{s'}$, and it follows by expanding Eq. (3) about $p = p_c$ and combining with Eq. (4) that, for p close to p_c and s large (see Refs. [31,32] for more details),

$$s^{\tau-2} P_{\geqslant s} \sim A_1[1 + B_1(p - p_c)s^\sigma + C_1 s^{-\Omega}]. \tag{5}$$

where A_1, B_1 and C_1 are nonuniversal constants.

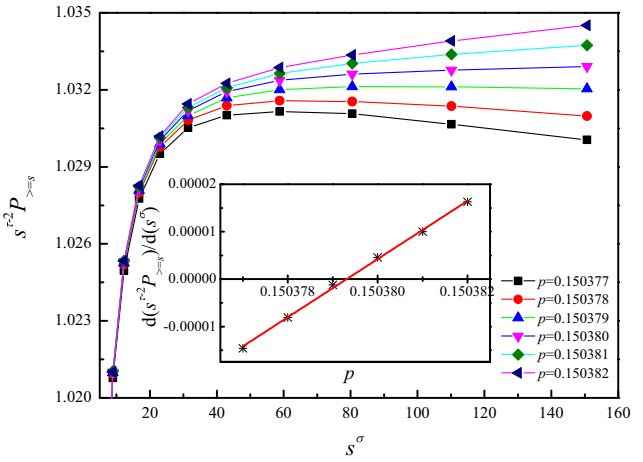

FIG. 3. Plot of $s^{\tau-2}P_{\geqslant s}$ vs s^σ with $\tau = 2.18905$ and $\sigma = 0.4522$ for the SC-1,4 lattice under different values of p. The inset indicates the slope of the linear portions of the curves shown in the main figure as a function of p, and the central value of $p_c = 0.1503793$ can be calculated from the p intercept.

III. RESULTS

A. Results in three dimensions

With regard to the universal exponents of τ, Ω, and σ, in three dimensions, relatively accurate and acceptable results are known: 2.18906(8) [38], 2.18909(5) [39] for τ, 0.64(2) [37], 0.65(2) [40], 0.60(8) [41], 0.64(5) [42] for Ω, and 0.4522(8) [38], 0.45237(8) [39], 0.4419 [43] for σ.

We set the upper size cutoff to be 2^{16} occupied sites. Monte Carlo simulations were performed on system size $L \times L \times L$ with $L = 512$ in three dimensions under periodic boundary conditions. Some 10^9 independent samples were produced for most of the lattices, except 3×10^8 when considering nth nearest neighbors with $n > 4$. We chose $\tau = 2.18905(15)$, $\Omega = 0.63(4)$, and $\sigma = 0.4522(2)$. Here we take large error bars on these values for the sake of safety. Then the number of clusters greater than or equal to size s could be found based on the data from our simulations, and the quantity $s^{\tau-2}P_{\geqslant s}$ could be easily calculated.

First, we can see from Eq. (5) that if we use s^σ as the abscissa and $s^{\tau-2}P_{\geqslant s}$ as ordinate, then Eq. (5) predicts that $s^{\tau-2}P_{\geqslant s}$ will convergence to a constant value at p_c for large s, while it deviates linearly from that constant value when p is away from p_c. Figure 3 shows the relation of $s^{\tau-2}P_{\geqslant s}$ versus s^σ for the SC-1,4 lattice under probabilities $p = 0.150377$, 0.150378, 0.150379, 0.150380, 0.150381, and 0.150382. A steep rise can be seen for small clusters, due to the finite-size-effect term ($s^{-\Omega}$). Then the plot shows a linear region for large clusters. The linear portion of the curve become more nearly horizontal when p is close to p_c. The central value of p_c can then be deduced using these properties

$$\frac{d(s^{\tau-2}P_{\geqslant s})}{d(s^\sigma)} \sim B_1(p - p_c), \tag{6}$$

as shown in the inset of Fig. 3, $p_c = 0.1503793$ can be calculated from the p intercept of the plot of the above derivative versus p.

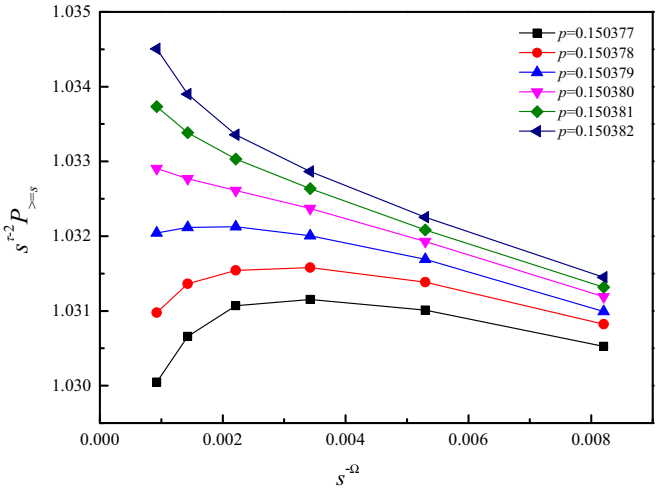

FIG. 4. Plot of $s^{\tau-2}P_{\geqslant s}$ vs $s^{-\Omega}$ with $\tau = 2.18905$ and $\Omega = 0.63$ for the SC-1,4 lattice under different values of p.

When p is very close to p_c, percolation thresholds can also be estimated based on the $s^{-\Omega}$ terms in Eq. (5). At $p = p_c$, there will be a linear relationship between $s^{\tau-2}P_{\geqslant s}$ and $s^{-\Omega}$ for large s, while for $p \neq p_c$ the behavior will be nonlinear. A plot of $s^{\tau-2}P_{\geqslant s}$ versus $s^{-\Omega}$ for the SC-1,4 lattice under probabilities $p = 0.150377$, 0.150378, 0.150379, 0.150380, 0.150381, and 0.150382, is shown in Fig. 4. Better linear behavior occurs when p is very close to p_c. If p is away from p_c, we can see the curves show an obvious deviation from linearity for large s. The range $0.150379 < p_c < 0.150380$ can be concluded here, which is consistent with the value we deduced from Fig. 3.

Comprehensively considering the two methods above, as well as the errors for the values of $\tau = 2.18905(15)$ and $\Omega = 0.63(4)$, we conclude the site percolation threshold of the SC-1,4 lattice to be $p_c = 0.1503793(7)$, where the number in parentheses represents the estimated error in the last digit.

The simulation results for the other 15 3D lattices we considered are shown in the Supplemental Material [44] in Figs. 1–30, and the corresponding thresholds are summarized in Table III.

B. Results in two dimensions

In two dimensions the universal exponents of $\tau = 187/91$, $\Omega = 72/91$, and $\sigma = 36/91$ are known exactly [2,46]. We again set upper size cutoff to be 2^{16} occupied sites. Monte Carlo simulations were performed on system size $L \times L$ with $L = 16\,384$ under periodic boundary conditions. More than 3×10^8 independent samples were produced for each lattice.

Figures 5 and 6 show the plots of $s^{\tau-2}P_{\geqslant s}$ versus s^{σ} and $s^{-\Omega}$, respectively, for the SQ-1, …,8 lattice under probabilities $p = 0.095763$, 0.095765, 0.095766, 0.095767, and 0.095769. Similar to the analysis process of thee dimensions, we deduce the site percolation threshold of the lattice here to be $p_c = 0.0957661(9)$. The simulation results for the other six 2D lattices we considered are shown in the Supplemental Material [44] in Figs. 31–42, and the corresponding thresholds are summarized in Table IV.

TABLE III. Site percolation thresholds for the simple cubic (SC) lattice with combinations of nearest neighbors up to the ninth nearest neighbors, showing the results found here and in previous works.

Lattice	z	p_c (present)	p_c (previous)
SC-1,4	12	0.1503793(7)	0.15040(12) [26]
SC-3,4	14	0.1759433(7)	0.175 [15], 0.1686 [17]
			0.20490(12) [26]
SC-1,3	14	0.1361470(10)	0.1420(1) [25]
SC-1,2	18	0.1373045(5)	0.136 [14], 0.137 [15]
			0.1372(1) [25]
SC-2,4	18	0.1361408(8)	0.15950(12) [26]
SC-1,3,4	20	0.1038846(6)	0.11920(12) [26]
SC-2,3	20	0.1037559(9)	0.1036(1) [25]
SC-1,2,4	24	0.0996629(9)	0.11440(12) [26]
SC-1, 2, 3	26	0.0976444(6)	0.097 [15], 0.0976(1) [25]
			0.0976445(10) [45]
SC-2,3,4	26	0.0856467(7)	0.11330(12) [26]
SC-1,2,3,4	32	0.0801171(9)	0.10000(12) [26]
SC-1, …,5	56	0.0461815(5)	–
SC-1, …,6	80	0.0337049(9)	0.033702(10) [11]
SC-1, …,7	92	0.0290800(10)	–
SC-1, …,8	122	0.0218686(6)	–
SC-1, …,9	146	0.0184060(10)	–

IV. DISCUSSION

A. Analysis of our results

In Tables III and IV, we compare our results with previous values, which are shown in the last column of each table. Our results here are at least two orders of magnitude more precise than most previous values. For some lattices, we get new thresholds that apparently were not studied before.

For several lattices in three dimensions, we find significant differences in the threshold values from those of Refs. [25] and [26]. There are several reasons to believe our values

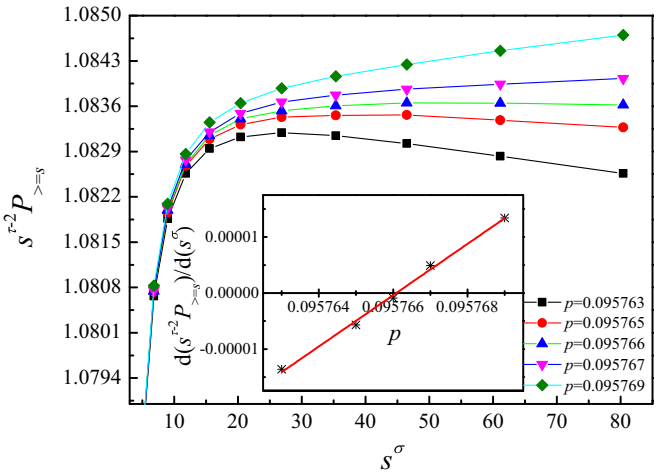

FIG. 5. Plot of $s^{\tau-2}P_{\geqslant s}$ vs s^{σ} with $\tau = 187/91$ and $\sigma = 36/91$ for the SQ-1, …, 8 lattice under different values of p. The inset indicates the slope of the linear portions of the curves shown in the main figure as a function of p, and the predicted value of $p_c = 0.0957661$ can be calculated from the p intercept.

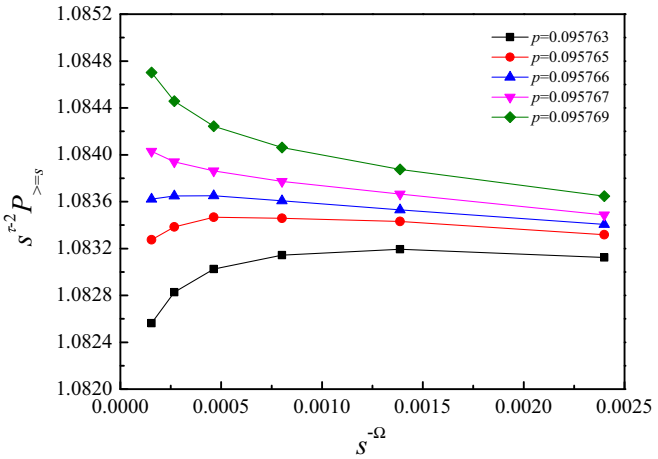

FIG. 6. Plot of $s^{\tau-2}P_{\geqslant s}$ vs $s^{-\Omega}$ with $\tau = 187/91$ and $\Omega = 72/91$ for the SQ-1, …, 8 lattice under different values of p.

are correct. For example, for the SC-1,2,3,4 lattice, we find $p_c = 0.0801171(9)$ compared to the value $p_c = 0.10000(12)$ given in Ref. [26]. But the latter cannot be correct as it is higher than the value ≈ 0.097 for the SC-1,2,3 lattice found by others as well as by us. If one neighborhood is a subset of another's, its threshold must be higher, not lower. Likewise, the threshold for SC-2,3,4 should be lower than that of SC-2,3, but it was found to be higher in Ref. [26]. Our results also make sense because they consistently follow the expected asymptotic scaling discussed below.

Our results in two dimensions are consistent with previous works. It is interesting to point out that the early series results of Dalton, Domb, and Sykes [14,15] are all substantially correct to the number of digits given (three), and the same is true of the work of d'Iribarne *et al.* [21]. Note that the model SQ-1,2 is just the matching lattice to site percolation on a simple square lattice, so its threshold is $1 - p_c^{\rm SQ} = 1 - 0.59274605\ldots$.

Some of the models considered here were previously studied by Koza *et al.* in the context of the percolation of overlapping objects on a lattice [11]. These authors considered squares of size $k \times k$ and cubes of size $k \times k \times k$, randomly distributed in an overlapping manner on square or cubic lattices. The critical number (per site) of these objects for percolation between neighboring occupied sites defines the

TABLE IV. Site percolation thresholds for the square (SQ) lattice with compact neighborhoods up to the eighth nearest neighbors.

Lattice	z	p_c (present)	p_c (previous)
SQ-1,2	8	0.4072531(11)	0.40725395 …[47]
SQ-1,2,3	12	0.2891226(14)	0.292 [15], 0.290(5) [16], 0.288 [24]
SQ-1,2,3,4	20	0.1967293(7)	0.196 [24] 0.196724(10) [45]
SQ-1, …,5	24	0.1647124(6)	0.164 [24], 0.163 [21]
SQ-1, …,6	28	0.1432551(9)	0.142 [21]
SQ-1, …,7	36	0.1153481(9)	0.113 [21]
SQ-1, …,8	44	0.0957661(9)	0.095765(10) [11], 0.095 [21]

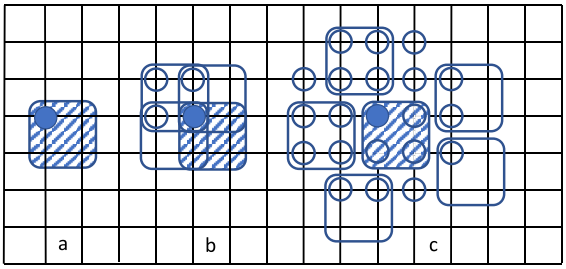

FIG. 7. Adsorption of a 2×2 object on a square lattice. (a) The object, showing the index site in one corner. (b) The four places where an object can cover the filled-in site. (c) The 20 places where additional objects can be placed that will overlap or border the shaded object; shown are the 20 index sites of those objects, and the outlines of some of them (after Ref. [11]).

threshold p_c. Thus, if you pick one point on each object, such as the center or a corner, as the "index site," then p_c is the number of these index sites divided by the total number of sites on the lattice at the critical point. An example of an index site for a 2×2 square is shown in Fig. 7(a).

We define $\phi(k)$ as the fraction of sites on the lattice covered by the squares or cubes, with a value $\phi_c(k)$ at the percolation point. This quantity can be related to p_c defined above by the following argument [11]: Consider an arbitrary lattice site in the system; that site will be covered by an object if there is any index site of any object within a region of volume k^d around that point, as shown in Fig. 7(b) for 2×2 objects in two dimensions. The probability that the site is empty is equal to the probability that there are no index sites within that region, $(1 - p_c)^{k^d}$. Consequently, the probability the site is occupied, which is just $\phi_c(k)$, is given by $\phi_c(k) = 1 - (1 - p_c)^{k^d}$. Solving for p_c, yields

$$p_c = 1 - (1 - \phi_c(k))^{1/k^d} \tag{7}$$

Values of $\phi_c(k)$ from [11] and the resulting p_c are given in Tables VII and VIII. Percolation of overlapping objects can be mapped to extended-range percolation between the index sites. The effective neighborhoods of those sites is determined by a simple geometric construction and is essentially the same shape as the object but twice as large [12]. In Fig. 7(c) we show the situation for a 2×2 object on a square lattice. There are 20 total sites (not counting the index site of the original object) corresponding to the index sites of additional objects that border or overlap the original object. Thus, this system is equivalent to an extended-range percolation problem with $z = 20$. The neighborhood can be seen to include up to the fourth nearest neighbors: SQ-1,2,3,4. The value $\phi_c(2) = 0.58365(2)$ found in Ref. [11] translates to $p_c = 0.196724(10)$, which is consistent with our value 0.1967293(7). Likewise, the overlap of 3×3 squares corresponds to extended-range percolation on the SQ-1, …,8 lattice with $z = 44$, and the value of Koza *et al.* $\phi_c(3) = 0.59586(2)$ corresponds to $p_c = 0.095765(10)$ compared to our measured value of 0.0957661(9). In three dimensions, Koza *et al.* find $\phi_c(2) = 0.23987(2)$ for $2 \times 2 \times 2$ objects, which corresponds to the SC-1, …,6 system with $z = 80$, and by Eq. (7) yields $p_c = 0.033702(10)$, compared to our value of 0.0337049(9). In general, for the overlap of k^d

squares and cubes on a lattice, the coordination number of the equivalent extended-range percolation problem is given by

$$z = \begin{cases} (2k+1)^2 - 5 & \text{(in two dimensions)} \\ (2k+1)^3 - 12(2k) + 3 & \text{(in three dimensions)} \end{cases}. \quad (8)$$

These formulas represent in two dimensions a square of dimension $2k+1$ with the corners missing, and in three dimensions a cube of dimension $2k+1$ with a column missing from each edge, as well as the center sites missing in both cases.

When k becomes large, these models limit to the percolation of aligned squares or cubes on a continuum, something that has also been studied precisely [33,48]. Then $\phi_c(k)$ limits to ϕ_c for the continuum systems. One also defines η_c as the total area or volume of the objects placed or adsorbed in the system, including the volume of the overlapped parts, divided by the volume of the system, and is related to ϕ_c by

$$\phi_c = e^{-\eta_c} \quad (9)$$

Note that η_c can be greater than 1, which is the case for most 2D systems, while $\phi_c < 1$ always. Koza *et al.* [11,12] consider an approximation to find p_c for k^d objects with large but finite k by replacing $\phi_c(k)$ by the continuum limit ϕ_c in Eq. (7). We will discuss this approximation more below.

B. Asymptotic behavior for large z

Here we generalize the discussion of the relation between percolation on a continuum and lattice percolation for neighborhoods of a general shape, to find a formula for the large-z behavior of p_c. This analysis will apply to the systems we studied with compact neighborhoods, which are all in two dimensions, and most in three dimensions.

We consider a continuum system of volume V with the random placement of N overlapping objects of a given shape. The continuum percolation threshold η_c represents the total volume fraction of the adsorbed objects, including the overlapping volume, at the critical point:

$$\eta_c = a_d r^d \frac{N}{V}, \quad (10)$$

where r is the radius or other length scale of the object and $a_d r^d$ is its volume, with a_d depending upon its shape. We use the terminology "adsorbed" to indicate that the object is placed or superimposed on the system. For example, for disks of radius r, $a_2 = \pi$, and for squares of side L we have $r = L/2$ and $a_2 = 4$. Covering the space occupied by the objects with a fine lattice, we see that the system maps to site percolation with extended neighbors of essentially the same shape but with a length scale $2r$ about the central point, because two objects of length scale r will just touch when the centers are separated a distance $2r$. (This is similar to the concept of a sphere of influence for hard-sphere systems in statistical mechanics.) Now the ratio N/V corresponds to the site occupation threshold p_c of index sites of the objects, assuming one index site per object and the total volume is just the total number of sites in the fine lattice. Thus we are assuming one unit of volume per site. For example, we saw in the previous section that the effective neighborhoods of squares of size k are squares of side $2k+1$ with the corners cut out, so those squares of influence are roughly twice as large as the object and roughly the same shape [Fig. 7(c)]. The effective z is equal to the number of sites within that region of influence of length scale $2r$, so that $z = a_d(2r)^d$, again assuming one unit of area per sites. (Note, technically z here should be $z+1$ because it should include the origin which is not counted as a nearest neighbor, but we ignore that difference here.) Then from Eq. (10) it follows that

$$zp_c = 2^d \eta_c, \quad (11)$$

This should describe the behavior of p_c for large z where the objects become similar to a continuum.

For circular neighborhoods in two dimensions, where η_c of a disk equals 1.128087 [33,48–51], one should thus expect from Eq. (11)

$$p_c = \frac{4.51235}{z}, \quad (12)$$

while for spherical neighborhoods in three dimensions, where η_c for spheres equals 0.34189 [52–54], one should expect

$$p_c = \frac{2.7351}{z}. \quad (13)$$

Interestingly, in Ref. [15], Domb and Dalton observed that for site percolation in three dimensions, $p_c \approx 2.7/z$, consistent with Eq. (13). In Ref. [13] Domb related that coefficient to continuum percolation threshold, which of course was not known to high precision at that time.

In Table V we show the values of zp_c under different coordination numbers both in two and three dimensions. As z increases, the values of zp_c show a trend of growth in general toward these predicted values.

TABLE V. Values of zp_c from our simulation results for the SC and SQ lattices with various compact neighborhoods.

Neighbors	zp_c (SC)	zp_c (SQ)
1,2	2.471481	3.258025
1,2,3	2.538754	3.469471
1,2,3,4	2.563747	3.934586
1,…,5	2.586164	3.953098
1,…,6	2.696392	4.011143
1,…,7	2.675360	4.152532
1,…,8	2.667969	4.213708
1,…,9	2.687276	–

C. Finite-z correction

We find that this finite-z effect can be accurately taken into account by assuming $p_c = c/(z+b)$ where b and c are constants. We can also write this relation as

$$z = c/p_c - b. \quad (14)$$

If we plot z versus $1/p_c$, one can directly get the value of c from the slope and $-b$ from the intercept. Figure 8 shows such a plot for the lattices we studied with compact neighborhoods. Indeed we find $c = 2.722$ (3D) and $c = 4.527$ (2D), both close to the predictions $c = 2^d \eta_c$ in Eqs. (12) and (13).

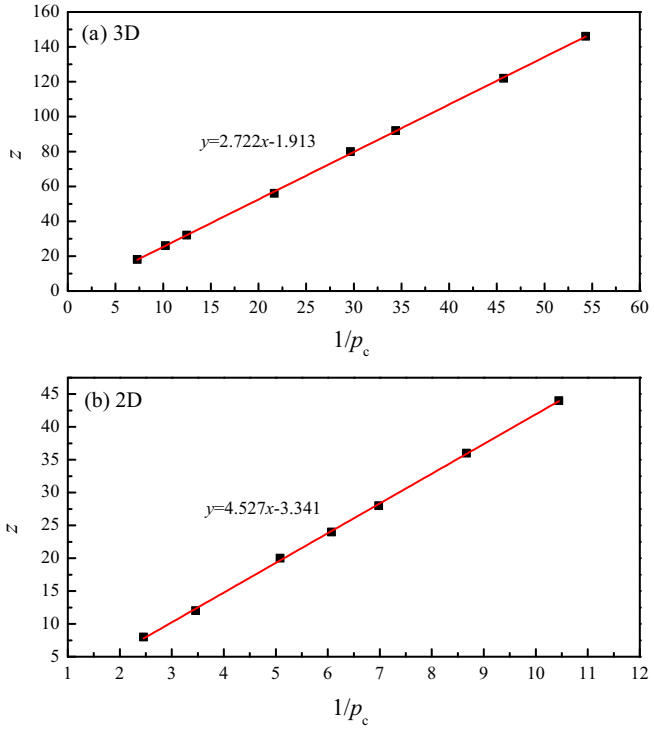

FIG. 8. Plots of z vs $1/p_c$ for the lattices with compact nearest neighborhoods: (a) Simple cubic lattice in three dimensions. The slope gives $c = 2.722$, compared with the prediction 2.7351 from Eq. (13). (b) Square lattice in two dimensions. The slope gives $c = 4.527$, compared with the prediction 4.51235 from Eq. (12).

To find this fitting form, we considered a variety of other plots, including p_c versus $1/z$, zp_c versus z^{-x}, $\ln p_c$ versus $\ln z$, etc. The plot of z versus $1/p_c$ seemed to give the best fit in both two and three dimensions, suggesting that adding a constant b to z is an accurate way to take into account the finite-z corrections to the asymptotic continuum percolation formula. The values of b vary somewhat and are sensitive to the number of points used in the fit. The main purpose of making these plots is to find a good estimate of the asymptotic value of $c = 2^d \eta_c$.

D. Analysis of other works

There have been several other works looking at site percolation on compact extended-range systems, and it is interesting to compare those results with those found here.

As mentioned above, some previous works involved extended-range systems with square and cubic neighborhoods. For the continuum percolation of aligned squares, one has $\eta_c = 1.0988428$ [48,53,55], which by Eq. (11) implies the asymptotic behavior

$$zp_c = 4\eta_c = 4.39537, \tag{15}$$

while for aligned cubes one has $\eta_c = 0.324766$ [12,56], implying

$$zp_c = 8\eta_c = 2.59813. \tag{16}$$

In a relatively early work, Gouker and Family [16] studied diamond-shaped neighborhoods (rotated squares) on a square lattice, with a lattice distance of R steps from the origin. In Table VI we show their results along with the corresponding z for each R. Their system for $R = 2$ corresponds to the SQ-1,2,3 system studied here and is included in Table IV. Figure 9 gives a plot of z versus $1/p_c$ and shows that their data are also consistent with our general form, Eq. (1). The neighborhood here is effectively a square rotated by 45°, and the slope 4.175 is obtained from the data fitting. This value is somewhat lower than the prediction in Eq. (15) but not inconsistent considering the relatively low precision of their results.

TABLE VI. Values of p_c for diamond-shaped neighborhoods on a SQ lattice of Gouker and Family [16] and the corresponding neighborhoods and z.

R	SQ neighbors	z	p_c	zp_c
2	1, 2, 3	12	0.29	3.48
4	1, 2, 3, 4, 5, 6, 7, 9	40	0.105	4.20
6	1, 2, 3, …, 13 (partial), 14, 18	84	0.049	4.12
8	…	144	0.028	4.03
10	…	220	0.019	4.18

More recently, Koza *et al.* [11] and Koza and Pola [12] studied overlapping squares, cubes, and higher-dimensional hypercubes. As discussed above, their results for a critical coverage fraction $\phi_c(k)$ can be translated to a site percolation threshold according to Eq. (7), with z given by Eq. (8). In Tables VII and VIII we give the results for p_c and z and plot them in Fig. 10. Data fittings give $c = 4.398$ for two dimensions, consistent with Eq. (15), and $c = 2.617$ for three dimensions, consistent with Eq. (16).

Very recently, Malarz [28] has studied site percolation on various neighborhoods on the triangular lattice, including hexagonal shells around the origin, which is somewhat analogous to the shells Gouker and Family considered on the square lattice. Previously, d'Iribarne *et al.* [21] had also studied this system with neighbors up to the 10th, to lower

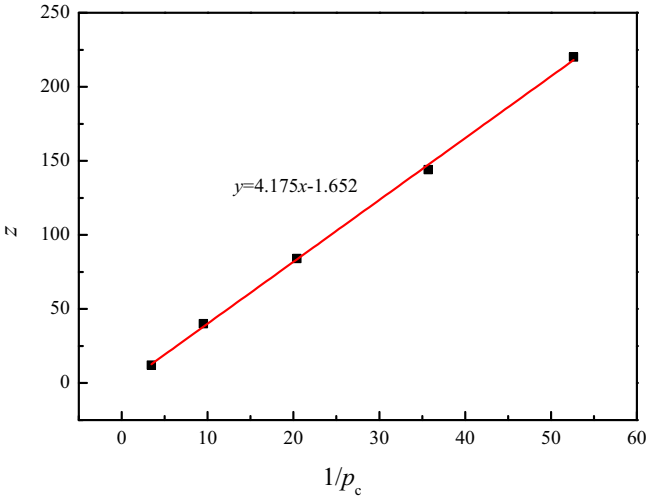

FIG. 9. Plot of z vs $1/p_c$ for the diamond-shaped neighborhood on a SQ lattice, with the lattice distance $R = 2$, 4, 6, 8, and 10 from left to right, using the data of Ref. [16]. The slope gives $c = 4.175$.

TABLE VII. Values of p_c for 2D systems related to the overlap of $k \times k$ objects on a SQ lattice, from Koza *et al.* [11]. Here p_c is deduced from ϕ_c using Eq. (7), and $z = 4k^2 + 4k - 4$ Eq. (8).

k	z	ϕ_c	p_c	zp_c
2	20	0.58365(2)	0.196724(10)	3.9345(2)
3	44	0.59586(2)	0.095765(10)	4.2137(2)
4	76	0.60648(1)	0.0566227(15)	4.3033(1)
5	116	0.61467(2)	0.037428(2)	4.3416(2)
7	220	0.62597(1)	0.0198697(5)	4.3713(1)
10	436	0.63609(2)	0.0100576(5)	4.3851(2)
20	1676	0.65006(2)	0.0026215(1)	4.3937(2)
100	40 396	0.66318(1)	0.000108815(6)	4.3957(2)
1000	4 003 996	0.66639(2)	1.0978×10^{-6}	4.3955(1)
10 000	400 039 996	0.66674(2)	1.0988×10^{-8}	4.3958(1)

precision. The data from both of these studies for hexagonal neighborhoods are shown in Table IX and the z versus $1/p_c$ plot is shown in Fig. 11. Again a good fit is seen. Note that the continuum threshold ϕ_c or η_c for aligned hexagons is not known, but presumably it is close to the case of disks, and indeed the value we find $c = 4.467$ is not far from the value 4.51235 predicted by Eq. (12) for disks. When we use just the three precise values of Malarz, we get $c = 4.517$. Finally, if we use the ten values of d'Iribarne *et al.*, which represents compact connection neighborhoods but of different shapes, we get $c = 4.434$, but with more scatter.

It is interesting to note that the threshold for the three-shelled hexagon TR-1, …,5, $p_c = 0.115740(36)$, with $z = 36$, is nearly identical to the threshold $p_c = 0.1153481(9)$ for SQ-1, …,7, which is in the shape of an octagon (see Fig. 1) and also has $z = 36$, showing that the coordination number z appears to be the principal determinant of the thresholds of systems with extended compact neighborhoods, with the lattice type and neighborhood shape seemingly less important.

E. Exponential form of finite-z behavior

Going back to the formula of Koza *et al.* Eq. (7), we recall that these authors proposed an approximation for large but finite z by replacing $\phi_c(k)$ by the continuum value ϕ_c, and

TABLE VIII. Values of p_c and zp_c deduced from the overlap of $k \times k \times k$ objects on a cubic lattice, from Koza *et al.* [11]. Here p_c is deduced from the Eq. (7) and $z = 8k^3 + 12k^2 - 18k + 4$, Eq. (8).

k	z	ϕ_c	p_c	zp_c
2	80	0.23987(2)	0.033702(3)	2.6962(3)
3	274	0.23436(1)	0.0098417(5)	2.6966(1)
4	636	0.23638(1)	0.0042050(2)	2.6744(1)
5	1214	0.23956(2)	0.0021885(2)	2.6568(3)
7	3210	0.24550(1)	0.00082095(4)	2.6352(1)
10	9024	0.25197(1)	0.00029027(1)	2.6194(1)
20	68 444	0.26246(2)	$3.8054(3) \times 10^{-5}$	2.6045(2)
100	8 118 204	0.27389(1)	$3.2005(1) \times 10^{-7}$	2.5983(1)
1000	8 011 982 004	0.27694(2)	$3.2426(3) \times 10^{-10}$	2.5978(2)
10 000	8.0012×10^{12}	0.27723(2)	$3.246(1) \times 10^{-13}$	2.5974(9)

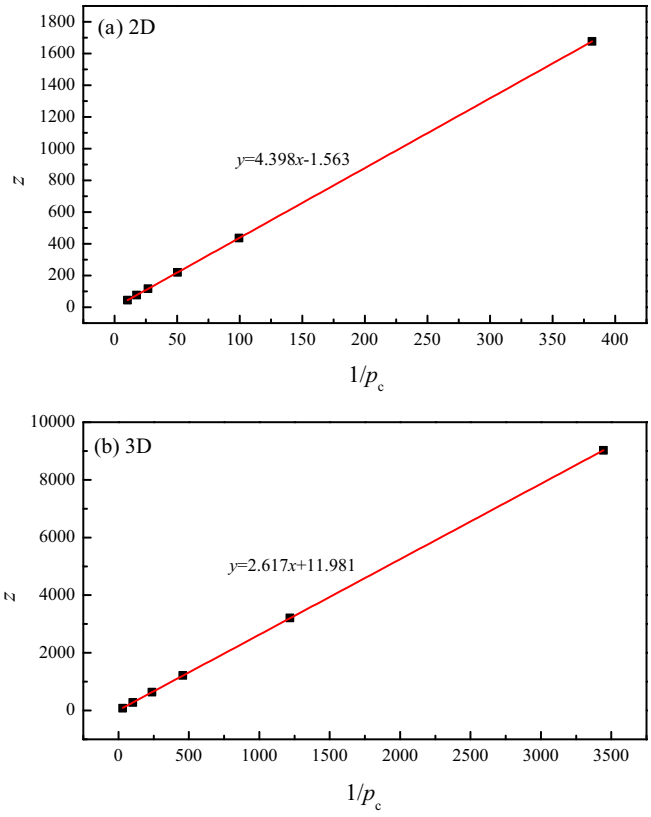

FIG. 10. Plots of z vs $1/p_c$ for (a) 2D systems related to the overlap of $k \times k$ objects on a SQ lattice for $k \leqslant 20$, and (b) 3D systems related to the overlap of $k \times k \times k$ objects on a SC lattice for $k \leqslant 10$, from the work of Koza *et al.* [11]. Here p_c is deduced from ϕ_c using Eq. (7). The slopes give $c = 4.398$ for two dimensions and $c = 2.617$ for three dimensions. The large value of b found in the 3D case is a artifact of the large range of z and is very sensitive to the number of points being used in the fit.

$(2k)^d$ by z, yielding

$$p_c = 1 - \exp(-2^d \eta_c / z) \tag{17}$$

To get this formula we also substituted $\phi_c = \exp(-\eta_c)$ by Eq. (9).

Now we suppose that this formula also applies to a system of any shape of neighborhoods, using the corresponding values of η_c and z for that system. This is because the derivation of Eq. (17) is essentially independent of the shape of the neighborhood. Note that this formula also does not depend upon the type of lattice (square, triangular, etc.)—all that

TABLE IX. Values of p_c for the triangular lattice (TR) with hexagonal-shaped neighborhoods, from Malarz [28] and d'Iribarne *et al.* [21].

Lattice	z	p_c from [28]	p_c from [21]
TR-1	6	0.500029(46)	0.500
TR-1,2,3	18	0.215484(19)	0.215
TR-1, …,5	36	0.115847(21)	0.115
TR-1, …,8	60		0.071

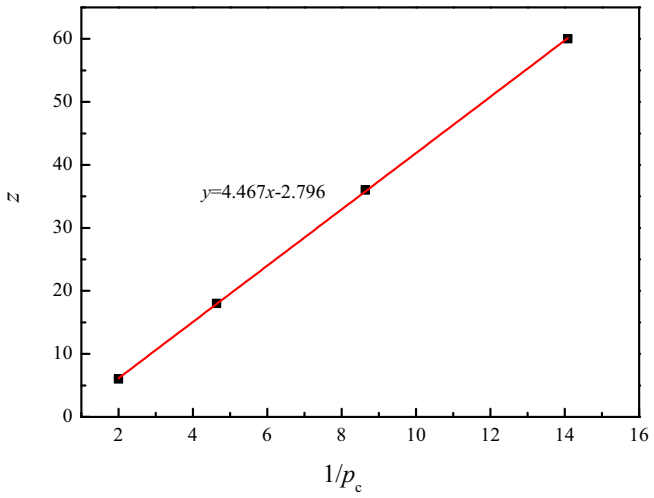

FIG. 11. Plot of z vs $1/p_c$ for the triangular lattice with compact hexagonal neighborhoods, from the work of Refs. [28] and [21]. The slope gives $c = 4.467$.

matters is the number of nearest neighbors z and the shape of the neighborhood which determines η_c. This is because for any lattice, for compact neighborhoods with z nearest neighbors, the number of sites in the equivalent object-adsorption problem is $(z/2)^d$. The area per lattice site effectively cancels out.

When z is large, Eq. (17) yields

$$zp_c = 2^d\eta_c - \frac{1}{2}\frac{(2^d\eta_c)^2}{z} + \cdots . \tag{18}$$

The leading term yields the asymptotic formula Eq. (11), and this represents another derivation of that result. The next-order term implies that b in Eq. (14) is given by $b = 2^{d-1}\eta_c = c/2$. This prediction does not agree accurately with the values we found, which suggests that this form Eq. (17) requires further corrections to accurately capture the finite-z corrections.

In Table X we show that, for various 2D compact systems, Eq. (17) gives better estimates for p_c than Eq. (11). Here we use η_c appropriate for disks. We also consider the results when replacing z by $z+1$, to account for the center site in calculating the effective area, and in general find even a better fit to the measured values. We note that Koza *et al.* also discuss additional corrections to their formula for squares and cubes, and perhaps these ideas apply to systems of other neighborhood shapes. Further investigation of this formula for different neighborhood shapes and dimensions is an area for future study.

F. Power-law fitting

Finally, we consider power-law fitting of the thresholds, since this has been considered in several other papers. Even though such fittings do not obey the necessary asymptotic behavior $\sim z^{-1}$, they are useful to give good estimates for finite-z systems. For example, in Ref. [25], it was found that the site thresholds for several 3D lattices can be fitted by $p_c(z) \sim z^{-a}$, with $a = 0.790(26)$. For bond percolation, it was found that $a = 1.087$ for many lattices in four dimensions [31] and $a = 1.111$ in three [32]. Other formulas have also been proposed to correlate percolation thresholds with z and other lattice properties [57–59], but we do not pursue them here.

TABLE X. Comparison of using Eqs. (11) and (17) to estimate p_c for some compact systems in two dimensions, with $\eta_c = 1.128087$ appropriate for disks. Data are from other tables in this paper. Note we have two systems with $z = 36$ and therefore identical estimates for p_c. In general, it can be seen that Eq. (17) gives much better results than Eq. (11). *The numbers with asterisks show the results when z is replaced by $z+1$ in both formulas, corresponding to including the origin in the number of sites. This substitution generally improves the overall accuracy of the results.

System	z	p_c	p_c, Eq. (11)	p_c, Eq. (17)
TR-1,2,3	18	0.215459(36)	0.25069	0.22173
			0.23749*	0.21140*
SQ-1,2,3,4	20	0.1967293(7)	0.22562	0.20198
			0.21487*	0.19336*
SQ-1, …,7	36	0.1153481(9)	0.12534	0.11781
TR-1, …,5	36	0.115740(36)	0.12196*	0.11481*
SQ-1, …,7,9	40	0.105	0.11281	0.10668
			0.11006*	0.10422*
SQ-1, …,8	44	0.0957661(9)	0.10255	0.097470
			0.10027*	0.095411*
TR-1, …,8	60	0.071	0.07521	0.07245
			0.07397*	0.07130*

Figure 12 shows a log-log plot of p_c versus z for lattices with compact nearest neighborhoods both in two dimensions

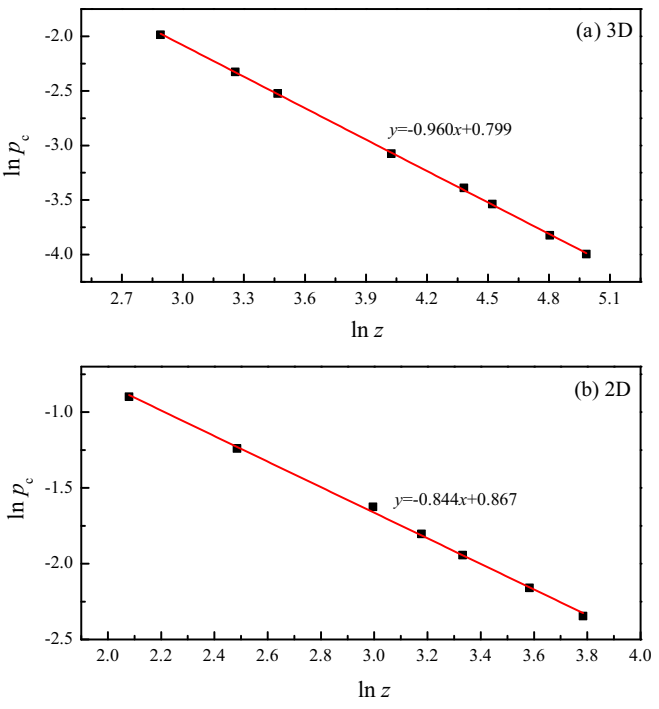

FIG. 12. Log-log plots of p_c vs z for the lattices with compact nearest neighborhoods: (a) Simple cubic lattice in three dimensions. The slope gives an exponent of $a = 0.960$, and the intercept ($z = 1$) of the line is at $\ln p_c = 0.799$. (b) Square lattice in two dimensions. The slope gives an exponent of $a = 0.844$, and the intercept of the line is at $\ln p_c = 0.867$.

and 3D. The percolation thresholds decrease monotonically with the coordination number, and linear behavior implies that the dependence of p_c on z follows a power law $p_c \sim cz^{-a}$. Data fittings lead to $a = 0.960$ for 3D site percolation and $a = 0.844$ for 2D site percolation.

V. CONCLUSIONS

To summarize, we have carried out extensive Monte Carlo simulations for site percolation on square and simple cubic lattices with various combinations of nearest neighbors, and found precise estimates of the percolation threshold for 16 3D systems and seven 2D systems, based upon an effective single-cluster growth method. Site percolation on lattices with some compact neighbors can be mapped to the problems of adsorption of extended objects on a lattice, such as disks and spheres, and also $k \times k \times k$ cubes (or $k \times k$ squares) on a cubic (or square) lattice as investigated by Koza *et al.* [11,12].

For large z, we predicted their continuum limits of $zp_c = 2.7351$ for 3D site percolation and $zp_c = 4.51235$ for 2D site percolation, by mapping to the percolation of overlapping spheres (or disks) in a continuum.

The finite-z effects in the simulation can be accurately taken into account by writing $(z + b)p_c = c$. The values of c that we found were consistent with the continuum percolation predictions $2^d \eta_c$. The values of b, which were found by the intercepts in our plots of z versus $1/p_c$, varied over a fairly wide range for different shaped neighborhoods, and are sensitive to the number of points used in the fit.

Another approach to the finite-z behavior can be found by generalizing the approach of Koza *et al.* to objects (and neighborhoods) of any shape, implying Eq. (17). We can get even better fits to the measurements by replacing z by $z + 1$. This intriguing formula deserves further study for neighborhoods of different shapes and in different dimensions.

We also looked at power-law correlations between site threshold and coordination number for the lattices with compact neighborhoods, and found that the thresholds decrease monotonically with the coordination number according to $p_c \sim cz^{-a}$, with the exponent $a = 0.960$ in three dimensions and $a = 0.844$ in two. While these power laws fit the data well in the range of the values of z we considered, they are not correct asymptotically for large z.

Some areas for future work include studying different lattices, including analyzing the extensive results of d'Iribarne *et al.* [21] for all 11 Archimedean lattices, looking at various shapes of neighborhoods (such as hexagons and octagons), and going to higher dimensions. This will help to understand the application of various approaches to fitting the data, such as Eqs. (1), (17), and (14) and power-law fits. Lattices with extended neighborhoods interpolate between discrete percolation and continuum percolation. Through the work of this paper, as well as former studies [13,28,31,60], one can have a deeper understanding of the relationship between these two limiting systems.

ACKNOWLEDGMENTS

The authors thank Hao Hu and Fereydoon Family for careful readings of this paper, and are grateful to the Advanced Analysis and Computation Center of CUMT for the award of CPU hours to accomplish this work. This work is supported by "the Fundamental Research Funds for the Central Universities" under Grant No. 2020ZDPYMS31.

[1] S. R. Broadbent and J. M. Hammersley, Percolation processes: I. Crystals and mazes, Math. Proc. Cambridge Philos. Soc. **53**, 629 (1957).

[2] D. Stauffer and A. Aharony, *Introduction to Percolation Theory*, 2nd ed. (CRC Press, Boca Raton, FL, 1994).

[3] S. F. Bolandtaba and A. Skauge, Network modeling of EOR processes: A combined invasion percolation and dynamic model for mobilization of trapped oil, Transp. Porous Media **89**, 357 (2011).

[4] V. V. Mourzenko, J.-F. Thovert, and P. M. Adler, Permeability of isotropic and anisotropic fracture networks, from the percolation threshold to very large densities, Phys. Rev. E **84**, 036307 (2011).

[5] C. L. Henley, Statics of a "Self-Organized" Percolation Model, Phys. Rev. Lett. **71**, 2741 (1993).

[6] N. Guisoni, E. S. Loscar, and E. V. Albano, Phase diagram and critical behavior of a forest-fire model in a gradient of immunity, Phys. Rev. E **83**, 011125 (2011).

[7] C. Moore and M. E. J. Newman, Epidemics and percolation in small-world networks, Phys. Rev. E **61**, 5678 (2000).

[8] R. M. Ziff, Percolation and the pandemic, Physica A **568**, 125723 (2021).

[9] J. M. Kleinberg, Navigation in a small world, Nature (London) **406**, 845 (2000).

[10] L. M. Sander, C. P. Warren, and I. M. Sokolov, Epidemics, disorder, and percolation, Physica A **325**, 1 (2003).

[11] Z. Koza, G. Kondrat, and K. Suszczyński, Percolation of overlapping squares or cubes on a lattice, J. Stat. Mech.: Theor. Exp. (2014) P11005.

[12] Z. Koza and J. Poła, From discrete to continuous percolation in dimensions 3 to 7, J. Stat. Mech.: Theor. Exp. (2016) 103206.

[13] C. Domb, A note on the series expansion method for clustering problems, Biometrika **59**, 209 (1972).

[14] N. W. Dalton, C. Domb, and M. F. Sykes, Dependence of critical concentration of a dilute ferromagnet on the range of interaction, Proc. Phys. Soc. **83**, 496 (1964).

[15] C. Domb and N. W. Dalton, Crystal statistics with long-range forces: I. The equivalent neighbor model, Proc. Phys. Soc. **89**, 859 (1966).

[16] M. Gouker and F. Family, Evidence for classical critical behavior in long-range site percolation, Phys. Rev. B **28**, 1449 (1983).

[17] G. R. Jerauld, L. E. Scriven, and H. T. Davis, Percolation and conduction on the 3D Voronoi and regular networks: A second case study in topological disorder, J. Phys. C: Solid State **17**, 3429 (1984).

[18] T. R. Gawron and Marek Cieplak, Site percolation thresholds of FCC lattice, Acta Phys. Pol. A **80**, 461 (1991).

[19] C. d'Iribarne, G. Rasigni, and M. Rasigni, Determination of site percolation transitions for 2D mosaics by means of the minimal spanning tree approach, Phys. Lett. A **209**, 95 (1995).

[20] C. d'Iribarne, M. Rasigni, and G. Rasigni, Minimal spanning tree and percolation on mosaics: Graph theory and percolation, J. Phys. A: Math. Gen. **32**, 2611 (1999).

[21] C. d'Iribarne, M. Rasigni, and G. Rasigni, From lattice long-range percolation to the continuum one, Phys. Lett. A **263**, 65 (1999).

[22] K. Malarz and S. Galam, Square-lattice site percolation at increasing ranges of neighbor bonds, Phys. Rev. E **71**, 016125 (2005).

[23] S. Galam and K. Malarz, Restoring site percolation on damaged square lattices, Phys. Rev. E **72**, 027103 (2005).

[24] M. Majewski and K. Malarz, Square lattice site percolation thresholds for complex neighbourhoods, Acta Phys. Pol. B **38**, 2191 (2007).

[25] Ł. Kurzawski and K. Malarz, Simple cubic random-site percolation thresholds for complex neighbourhoods, Rep. Math. Phys. **70**, 163 (2012).

[26] K. Malarz, Simple cubic random-site percolation thresholds for neighborhoods containing fourth-nearest neighbors, Phys. Rev. E **91**, 043301 (2015).

[27] M. Kotwica, P. Gronek, and K. Malarz, Efficient space virtualization for the Hoshen-Kopelman algorithm, Int. J. Mod. Phys. C **30**, 1950055 (2019).

[28] K. Malarz, Site percolation thresholds on triangular lattice with complex neighborhoods, Chaos **30**, 123123 (2020).

[29] Y. Ouyang, Y. Deng, and H. W. J. Blöte, Equivalent-neighbor percolation models in two dimensions: Crossover between mean-field and short-range behavior, Phys. Rev. E **98**, 062101 (2018).

[30] Y. Deng, Y. Ouyang, and H. W. J. Blöte, Medium-range percolation in two dimensions, J. Phys.: Conf. Ser. **1163**, 012001 (2019).

[31] Z. Xun and R. M. Ziff, Precise bond percolation thresholds on several four-dimensional lattices, Phys. Rev. Research **2**, 013067 (2020).

[32] Z. Xun and R. M. Ziff, Bond percolation on simple cubic lattices with extended neighborhoods, Phys. Rev. E **102**, 012102 (2020).

[33] W. Xu, J. Wang, H. Hu, and Y. Deng, Critical polynomials in the nonplanar and continuum percolation models, Phys. Rev. E **103**, 022127 (2021).

[34] S. Frei and E. Perkins, A lower bound for p_c in range-r bond percolation in two and three dimensions, Electron. J. Probab. **21**, 56 (2016).

[35] M. Lang and T. Müller, Analysis of the gel point of polymer model networks by computer simulations, Macromolecules **53**, 498 (2020).

[36] X. Feng, Y. Deng, and H. W. J. Blöte, Percolation transitions in two dimensions, Phys. Rev. E **78**, 031136 (2008).

[37] C. D. Lorenz and R. M. Ziff, Precise determination of the bond percolation thresholds and finite-size scaling corrections for the sc, fcc, and bcc lattices, Phys. Rev. E **57**, 230 (1998).

[38] H. G. Ballesteros, L. A. Fernández, V. Martín-Mayor, A. Muñoz Sudupe, G. Parisi, and J. J. Ruiz-Lorenzo, Measures of critical exponents in the four-dimensional site percolation, Phys. Lett. B **400**, 346 (1997).

[39] X. Xu, J. Wang, J.-P. Lv, and Y. Deng, Simultaneous analysis of three-dimensional percolation models, Front. Phys. **9**, 113 (2014).

[40] J.-C. Gimel, T. Nicolai, and D. Durand, Size distribution of percolating clusters on cubic lattices, J. Phys. A: Math. Gen. **33**, 7687 (2000).

[41] D. Tiggemann, Simulation of percolation on massively-parallel computers, Int. J. Mod. Phys. C **12**, 871 (2001).

[42] H. G. Ballesteros, L. A. Fernández, V. Martín-Mayor, A. Muñoz Sudupe, G. Parisi, and J. J. Ruiz-Lorenzo, Scaling corrections: Site percolation and Ising model in three dimensions, J. Phys. A: Math. Gen. **32**, 1 (1999).

[43] J. A. Gracey, Four loop renormalization of ϕ^3 theory in six dimensions, Phys. Rev. D **92**, 025012 (2015).

[44] See Supplemental Material at http://link.aps.org/supplemental/10.1103/PhysRevE.103.022126 for the simulation results.

[45] R. M. Ziff and S. Torquato (unpublished).

[46] R. M. Ziff, Correction-to-scaling exponent for two-dimensional percolation, Phys. Rev. E **83**, 020107(R) (2011).

[47] J. L. Jacobsen, Critical points of Potts and O(N) models from eigenvalue identities in periodic Temperley-Lieb algebras, J. Phys. A: Math. Theor. **48**, 454003 (2015).

[48] S. Mertens and C. Moore, Continuum percolation thresholds in two dimensions, Phys. Rev. E **86**, 061109 (2012).

[49] J. A. Quintanilla and R. M. Ziff, Asymmetry in the percolation thresholds of fully penetrable disks with two different radii, Phys. Rev. E **76**, 051115 (2007).

[50] Y. Yu. Tarasevich and A. V. Eserkepov, Percolation thresholds for discorectangles: Numerical estimation for a range of aspect ratios, Phys. Rev. E **101**, 022108 (2020).

[51] J. Li and M. Ostling, Precise percolation thresholds of two-dimensional random systems comprising overlapping ellipses, Physica A **462**, 940 (2016).

[52] C. D. Lorenz and R. M. Ziff, Precise determination of the critical percolation threshold for the three-dimensional "Swiss cheese" model using a growth algorithm, J. Chem. Phys. **114**, 3659 (2001).

[53] S. Torquato and Y. Jiao, Effect of dimensionality on the continuum percolation of overlapping hyperspheres and hypercubes. II. Simulation results and analyses, J. Chem. Phys. **137**, 074106 (2012).

[54] G. Gori and A. Trombettoni, Conformal invariance in three dimensional percolation, J. Stat. Mech.: Theor. Exp. (2015) P07014.

[55] D. R. Baker, G. Paul, S. Sreenivasan, and H. Eugene Stanley, Continuum percolation threshold for interpenetrating squares and cubes, Phys. Rev. E **66**, 046136 (2002).

[56] E. Hyytia, J. Virtamo, P. Lassila, and J. Ott, Continuum percolation threshold for permeable aligned cylinders and opportunistic networking, Commun. Lett. IEEE **16**, 1064 (2012).

[57] S. Galam and A. Mauger, Universal formulas for percolation thresholds, Phys. Rev. E **53**, 2177 (1996).

[58] S. C. van der Marck, Calculation of percolation thresholds in high dimensions for FCC, BCC and diamond lattices, Int. J. Mod. Phys. C **9**, 529 (1998).

[59] J. C. Wierman and D. P. Naor, Criteria for evaluation of universal formulas for percolation thresholds, Phys. Rev. E **71**, 036143 (2005).

[60] Z. Koza, Critical $p = 1/2$ in percolation on semi-infinite strips, Phys. Rev. E **100**, 042115 (2019).